DOI: 10.1002/chem.200903049

Self-Assembly of Calix[6]arene–Diazapyrenium Pseudorotaxanes: Interplay of Molecular Recognition and Ion-Pairing Effects

Monica Semeraro,[a] Arturo Arduini,[b] Massimo Baroncini,[a] Raffaella Battelli,[a] Alberto Credi,[a] Margherita Venturi,[a] Andrea Pochini,[b] Andrea Secchi,*[b] and Serena Silvi*[a]

Abstract: The calix[6]arene wheel **CX** forms pseudorotaxane species with the diazapyrenium-based axle **1**·2PF_6 in CH_2Cl_2 solution. The macrocyclic component is a heteroditopic receptor, which can complex the electron-acceptor moiety of the axle inside its cavity and the counterions with the ureidic groups on the upper rim. The self-assembled supramolecular species is a complex structure, which involves three components—the wheel, the axle and its counterions—that can mutually interact and affect. The stoichiometry of the resulting supramolecular complex depends on the nature and concentration of the counterions. Namely, it is observed that in dilute solution and with low-coordinating anions the axle takes two wheels, whereas with highly coordinating anions or in concentrated solutions the complex has a 1:1 stoichiometry.

Keywords: calixarenes · ion pairs · molecular devices · pseudorotaxanes · supramolecular chemistry

Introduction

Pseudorotaxanes are supramolecular systems minimally composed of an axle-like molecule surrounded by a macrocyclic component.[1] These peculiar host–guest systems represent convenient precursors for the synthesis of more complex interlocked structures, such as rotaxanes and catenanes,[1,2] which can operate as simple molecular machines. Essentially, the functioning mode of a pseudorotaxane consists of an external stimulus-promoted reversible threading–dethreading process. The structural information stored in both axle and wheel should match (be complementary) from a dimensional point of view as well as for the inter-component interactions responsible for the stability of the complex. A common feature of these systems is that the macrocycle resides in a precise position (station) along the axle, which is also the structural unit that responds to the external stimuli governing the dethreading–threading process. Typically this unit is positioned in a more or less central portion of the axial component. In a rotaxane, the two stoppers present at the termini of the axial component, by acting as a structural tie, prevent dethreading.

The ability of these systems to perform functions relies on their rational design, which in turn requires a deep knowledge of the interactions that occur among the molecular components. As the inter-component interactions that drive the recognition are electrostatic in nature, low-polarity solvents are frequently employed to maximize the efficiency of the self-assembly process. In many types of pseudorotaxanes, however, one of the components (usually the axle) is a charged species that is subject to ion pairing in apolar media.[3,4] Such ion-pairing equilibria can strongly affect the threading reaction, thereby complicating the rationalization of the self-assembly process.[4a–c] In the case of a charged axle, these effects can be circumvented or even advantageously exploited to improve the efficiency of the host–guest recognition process, by utilizing a heteroditopic macrocyclic component, which can simultaneously bind the guest and its counterions.[5]

[a] M. Semeraro, M. Baroncini, R. Battelli, Prof. A. Credi, Prof. M. Venturi, Dr. S. Silvi
Dipartimento di Chimica "G. Ciamician"
Università di Bologna
Via Selmi 2, 40126 Bologna (Italy)
Fax: (+39) 051 2099456
E-mail: serena.silvi@unibo.it

[b] Prof. A. Arduini, Prof. A. Pochini, Dr. A. Secchi
Dipartimento di Chimica Organica e Industriale
Università di Parma
via G.P. Usberti 17/a, 43100 Parma (Italy)
Fax: (+39) 0521905472
E-mail: andrea.secchi@unipr.it

Supporting information for this article is available on the WWW under http://dx.doi.org/10.1002/chem.200903049.

We have recently studied the ability of the tris(phenylureido)calix[6]arene **CX** to act as a heteroditopic and non-symmetrical wheel to form oriented pseudorotaxanes with

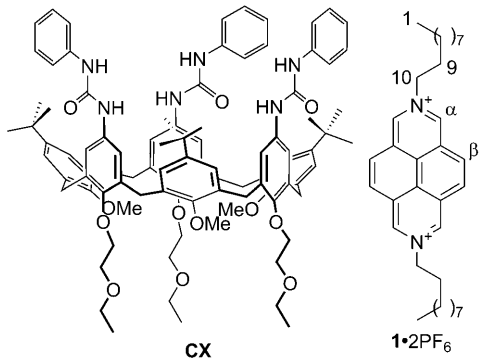

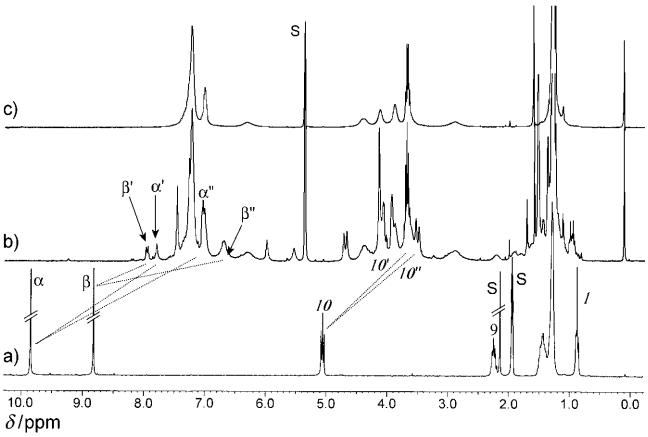

Figure 1. ^{1}H NMR stack plot (300 MHz) of: a) **1**·2PF$_6$ in CD_3CN; b) a mixture of **CX** and **1**·2PF$_6$ in CD_2Cl_2 (the dotted lines indicate a few representative resonances of $\mathbf{1}^{2+}$ that are up-field shifted upon complexation) and c) **CX** in CD_2Cl_2.

non-symmetrical 1,1′-dialkyl-4,4′-bipyridinium axles.[6] This three-dimensional macrocycle possesses a π-electron-donor cavity that can interact with electron-accepting positively charged units, and three efficient hydrogen-bonding donor phenylureido groups at the upper rim that, besides extending the cavity, can complex the counterions of the cationic axle, thus assisting its insertion into the wheel from this rim. By exploiting these peculiar binding properties, rotaxanes characterized by the unidirectional orientation of the two stoppers of the dumbbell with respect to the two calixarene rims were realized.[7]

Along this line, we envisaged that the electron-accepting dication 2,7-diazapyrenium (DAP) unit present in the *N*,*N*′-didecyl-2,7-diazapyrenium axle-like molecule **1**·2PF$_6$ (proton labelling as shown), because of its large size, could serve both as stopper and station (act as an active stopper) for the construction of pseudorotaxanes that can thread and dethread only from one side of the wheel. In addition, because of its spectroscopic features, it could also signal its proximity to a specific rim of the calixarene wheel. In fact, the DAP unit of compound $\mathbf{1}^{2+}$, like the previously studied 4,4′-bipyridinium moiety, is a cationic species that has already been used as the guest in supramolecular inclusion complexes;[8] $\mathbf{1}^{2+}$ has an extended π delocalization that confers characteristic spectroscopic features to this chromophore.[9] Its sharp, intense and structured absorption and luminescence bands can be easily monitored to reveal any alteration in the surrounding environment. The aim of this work is to study the self-assembly process of compounds $\mathbf{1}^{2+}$ and **CX**, and to investigate the parameters that affect pseudorotaxane formation.

Results and Discussion

NMR spectroscopic characterization: The ^{1}H NMR spectrum of **1**·2PF$_6$ taken in CD_3CN (see Figure 1a) shows a singlet at $\delta = 9.88$ ppm for the four aromatic α protons and a singlet at $\delta = 8.85$ ppm for the four β protons. The two equivalent methylene protons *10* resonate as a triplet at $\delta = 5.09$ ppm, whereas all other protons of the two alkyl chains resonate in the 2.3–0.8 ppm range. **1**·2PF$_6$ is not sufficiently soluble in low-polarity media for accurate NMR analysis; however, by adding a slight excess of the salt to solution of **CX** in $CDCl_3$, C_6D_6 or CD_2Cl_2, the appearance of a reddish colour of the solution suggests that in all instances a binding process between **1**·2PF$_6$ and **CX** has taken place. In CD_2Cl_2 the ^{1}H NMR spectrum showed sharper signals than those obtained in the other solvents, so it was selected to study the structure of the species present in solution and the stoichiometry of binding. The spectrum of the sample obtained after filtration of a 10 mM solution of **CX** containing an equivalent amount of **1**·2PF$_6$ clearly shows the presence of uncomplexed **CX** (see Figure 1c for the spectrum of free **CX**) together with a 1:1 adduct **CX**⊃**1**·2PF$_6$ (see Figure 1b).

Upon binding, **CX** adopts a pseudo-cone conformation as shown, for example, by the presence of an AX system at $\delta =$ 4.70 and 3.51 ppm for the six axial and six equatorial methylene protons of the bridges, respectively. The methoxy groups, which in the free wheel resonate as a very broad signal at $\delta \approx 3$ ppm, in the complex are visible as a down-field-shifted sharp singlet at $\delta \approx 4.14$ ppm, thus suggesting their guest-induced expulsion from the interior of the cavity.[6,7] The binding also appreciably affects the resonances of the guest protons as seen, for example, by the large up-field shift experienced by the signals of protons α and β belonging to the DAP unit. The former of these two signals splits into two singlets at $\delta = 7.79$ (α′) and 7.05 ppm (α″), whereas the latter splits into two doublets at $\delta = 7.95$ (β′) and 6.7 ppm (β″) with a coupling constant of 9 Hz (see Figure 1b). The signals of protons α″ and β″ were overlapped by more intense signals arising from the aromatic protons of **CX**. Their full assignment was thus accomplished through 2D COSY and HSQC experiments (see Figures S2 and S3 in the Supporting Information). The methylene groups *10* give

rise to two very broad signals at $\delta = 3.7$ (*10′*) and 3.6 ppm (*10″*). Both signals are up-field shifted ($\Delta\delta$ up to 1.5 ppm) with respect to the free **1**·2PF$_6$ (cf. Figure 1a and b) and are fully overlapped by stronger resonances arising from the 2-ethoxy–ethoxy chains present on the calix[6]arene lower rim. Nevertheless, their nature was verified through 2D COSY and TOCSY experiments (see Figures S2 and S4 in the Supporting Information).

The analysis of the integrals of the spectrum clearly supports the formation of an adduct with a 1:1 stoichiometry as the main host–guest complex. However, the variations of chemical shift observed for both **CX** and $\mathbf{1}^{2+}$ could be consistent with different structures of the complex. Namely, a pseudorotaxane structure in which one of the two alkyl chains of $\mathbf{1}^{2+}$ protrudes from the lower rim of the wheel (see Scheme 1a) or one in which the DAP unit of $\mathbf{1}^{2+}$ seats

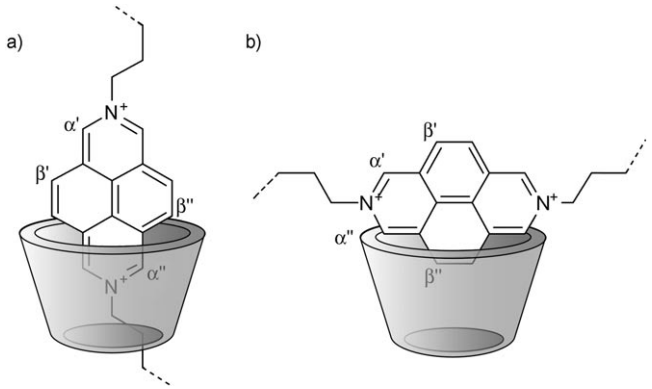

Scheme 1. Schematic representation of the two possible structures of the complex formed between the axle **1**·2PF$_6$ and wheel **CX**.

orthogonally to the upper rim of the calix[6]arene (Scheme 1b). The large up-field shift experienced by the resonances of α″ ($\Delta\delta \approx 2.8$ ppm) and β″ ($\Delta\delta \approx 2.1$ ppm) protons supports the hypothesis that a pseudorotaxane complex has formed in solution. In this structural arrangement, indeed, one part of the DAP unit is engulfed in the aromatic cavity of **CX**, thus exposing its protons to a more intense anisotropic shielding effect.

The small chemical shift differentiation endured by *10′* and *10″* could be explained by considering that, differently from what was previously observed for 1,1′-dialkyl-4,4′-bipyridinium-based axles,[6,7] the DAP unit of $\mathbf{1}^{2+}$, because of its size, is less engulfed in the aromatic cavity of the macrocycle and cannot protrude from its lower rim. This could impose on the two methylene groups *10′* and *10″* a similar anisotropic shielding effect, exerted by the calix[6]arene cavity and the phenyl groups present on the upper rim of **CX**. The threading reaction also accounts for the coupling observed between protons β′ and β″, which are no longer magnetically equivalent. 2D ROESY experiments of the complex finally confirmed the hypothesis, since there are several NOE cross-peaks arising from the spatial proximity between, for example, the methoxy groups present on the lower rim of **CX** and the methylene groups belonging to only one alkyl chain of $\mathbf{1}^{2+}$, and also between the β′ protons of DAP and the *tert*-butyl groups present on the upper rim of the macrocycle (see Figure S5 in the Supporting Information).

A few weak signals present in the spectrum of the 1:1 axle–wheel mixture of Figure 1b could not be assigned either to the pseudorotaxane adduct **CX**⊃**1**·2PF$_6$ or to the free **CX**. We formulated the hypothesis that these signals could arise from the formation of axle–wheel adducts having a stoichiometry higher than 1:1. To disclose the nature of all the species present in dichloromethane solution, some diffusion-ordered spectroscopy (DOSY) experiments were carried out (see the Experimental Section).[10,11] A mean diffusion coefficient D of $(0.68 \pm 0.02) \times 10^{-5}$ cm^{2}s^{-1} for **CX** was calculated by performing the NMR diffusion experiment on a 10 mM solution of the free **CX** in CD_2Cl_2. The experiment was then repeated under the same experimental conditions on the mixture containing **CX**⊃**1**·2PF$_6$ and yielded values of D that, depending on the resonance selected, ranged between 0.55 and 0.65×10^{-5} cm^{2}s^{-1}. The highest values were assigned to the resonances of the free **CX**, whereas the attenuation profiles of all resonances previously assigned to the pseudorotaxane, such as β′ (○) and α′ (▼; see Figure 2), afforded diffusion coefficients ranging from 0.56 to 0.58×10^{-5} cm^{2}s^{-1}.

The simple relationship $MW_{(1)}/MW_{(2)} = (D_{(2)}/D_{(1)})^3$ derived from the Stokes equation correlates the molecular weight

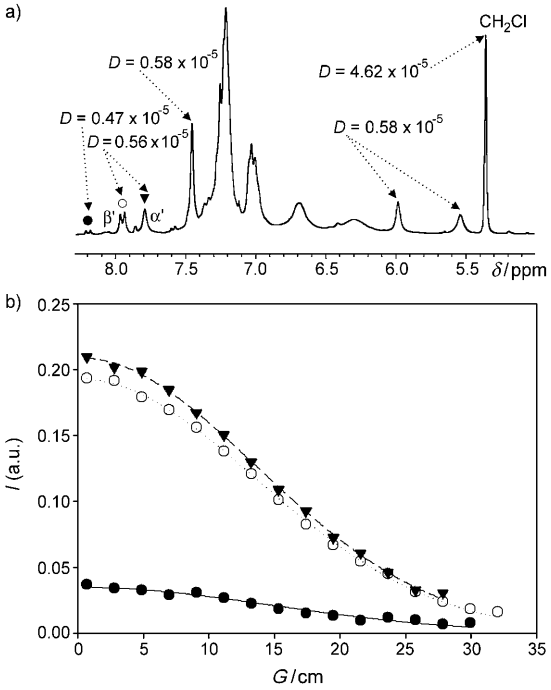

Figure 2. a) Expansion of the ^{1}H NMR spectrum (300 MHz) of a mixture containing the pseudorotaxane complex **CX**⊃**1**·2PF$_6$. The diffusion coefficients D calculated through NMR diffusion experiments are reported above the most representative peaks. b) Plot of the intensity attenuation profiles of resonances ●, ○ and ▼ upon gradient variation.

(MW) and the diffusion coefficient of two spherical species, (1) and (2), diffusing in solution under the same experimental conditions. The application of this equation to the diffusion data measured from the resonances of the pseudorotaxane yielded, despite the non-spherical shape of the diffusing species, a molecular weight range between 2360 and 2620 Da, which is in good agreement with the theoretical value of 2241 Da.[12] Very interestingly, the fitting of the attenuation profile of the weak doublet at $\delta = 8.2$ ppm (●, see Figure 2a) yielded an unexpectedly low value of D ($(0.47 \pm 0.04) \times 10^{-5}$ $cm^2 s^{-1}$). This value, though inaccurate, was an indication that in dichloromethane solution the formation of adducts having a stoichiometry higher than 1:1 is possible.

ESIMS experiments: To determine the nature of these higher-stoichiometry adducts, the previous mixture was submitted to high-resolution ESIMS analysis (see the Experimental Section). The spectrum recorded in the 700–2000 mass range (see Figure 3) shows the presence of a peak at m/z 1709.01 for the doubly charged 2:1 adduct $[(\mathbf{CX})_2 \supset \mathbf{1}]^{2+}$, along with the wheel **CX** (visible as the adduct with Na^+) and the most abundant doubly charged 1:1 adduct $[\mathbf{CX} \supset \mathbf{1}]^{2+}$ at m/z 976.10. Singly charged adducts that should retain at least one PF_6^- anion were never observed.

UV/Vis spectroscopic experiments: All photophysical experiments were performed in air-equilibrated CH_2Cl_2 solution at room temperature. The absorption and fluorescence spectra of compound $\mathbf{1}^{2+}$ show the typical[9] structured bands of the DAP chromophoric unit. The calixarene wheel **CX** shows an intense absorption band in the UV region of the spectrum and a weak luminescence (see Figure S6 in the Supporting Information and Table 1).

Table 1. Absorption and emission data for **CX** and **1**·2PF_6 (CH_2Cl_2, 293 K).

Compound	λ_{max} [nm]	$\varepsilon \times 10^{-3}$ [$M^{-1} cm^{-1}$]	λ_{em} [nm]	Φ	τ [ns]
	258	58			
1·2PF_6	338	35	427	0.39	7.7
	421	15			
CX	250	54	330	0.003	<1

To investigate the complexation equilibrium between **1**·2PF_6 and **CX**, we performed UV/Vis titration experiments. The addition of increasing amounts of the wheel component to the DAP-based thread caused remarkable changes in both the absorption (Figure 4) and emission spectra of **1**·2PF_6 [experiment (i)], namely, the absorption bands of the transition to the first $\pi\pi^*$ excited state ($350 < \lambda < 450$ nm) shifted to longer wavelengths, the bands corresponding to the transition to the second $\pi\pi^*$ excited state ($300 < \lambda < 350$ nm) broadened and weakened, and a broad absorption tail at $\lambda > 450$ nm appeared; the luminescence of the DAP moiety was quenched.

The absorption and luminescence data were fitted with the SPECFIT program,[13] which optimizes the interpolation

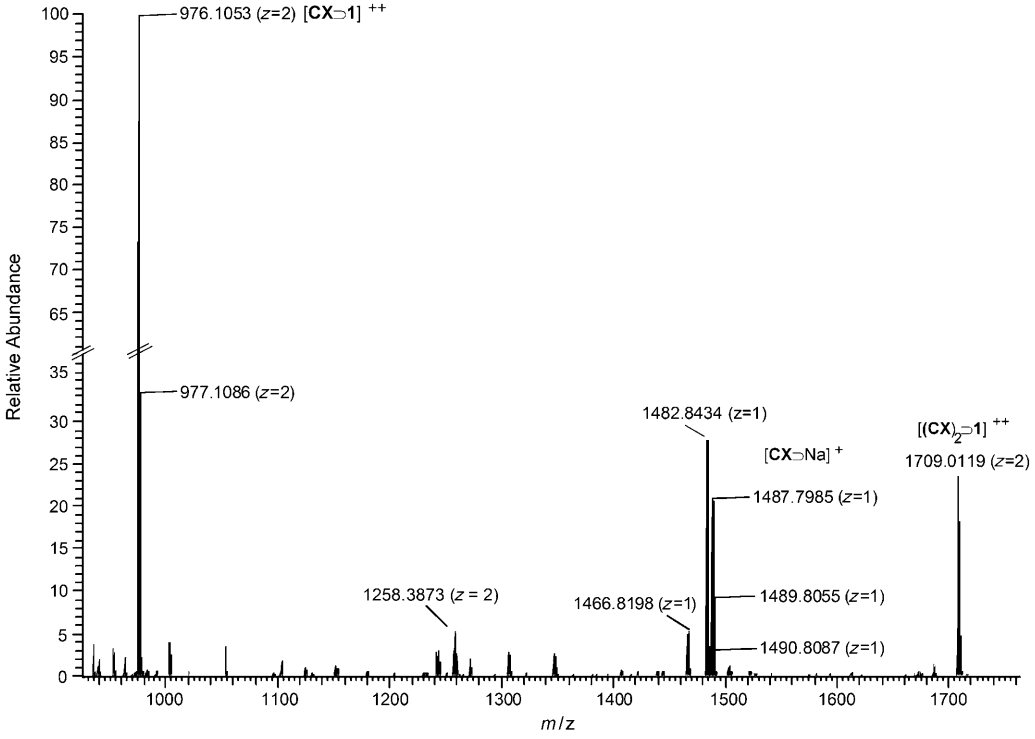

Figure 3. ESIMS spectrum of a mixture of **CX** and **1**·2PF_6 in 1:1 CH_2Cl_2/MeOH showing the doubly charged ($z = 2$) 1:1 $[\mathbf{CX} \supset \mathbf{1}]^{2+}$ and 2:1 $[(\mathbf{CX})_2 \supset \mathbf{1}]^{2+}$ adducts.

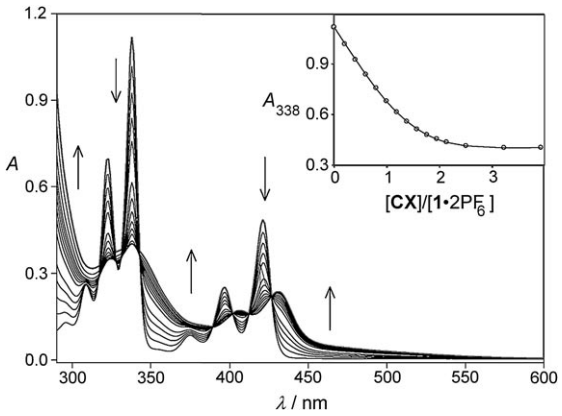

Figure 4. Absorption spectra of compound **1**·2PF$_6$ (3.3×10^{-5} M) upon titration with **CX**, CH_2Cl_2, RT. The inset shows the absorption changes at 338 nm (○) and the fitting curve (——) obtained by means of the SPECFIT fitting program.

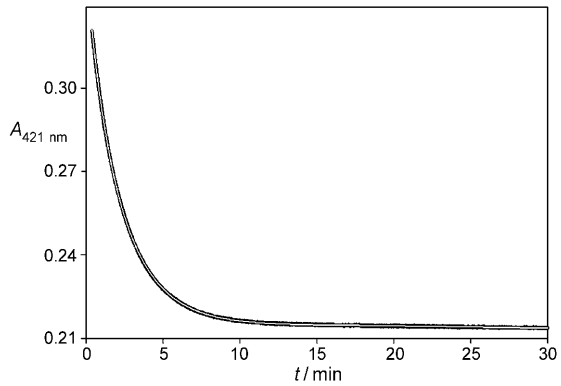

Figure 5. Kinetic trace (black line), recorded in CH_2Cl_2 at 293 K, for the absorbance changes at 421 nm obtained upon mixing **CX** (5.3×10^{-5} M) and **1**·2PF$_6$ (2.5×10^{-5} M). The white line is the fitting curve obtained by means of the SPECFIT fitting program.

of the titration data according to a given complexation model utilizing the whole investigated spectral range. The best fit was obtained by assuming the formation of both the 1:1 and 2:1 host–guest complexes [Table 2, experiment (i)].

Table 2. Thermodynamic and kinetic constants (CH_2Cl_2, RT).

Expt.	$K_1\times10^{-5}$ [M^{-1}][a]	$K_2\times10^{-5}$ [M^{-1}][b]	$k_1\times10^{-2}$ [M^{-1}s^{-1}][c]	$k_1'\times10^{3}$ [s^{-1}][c]	$k_2\times10^{-2}$ [M^{-1}s^{-1}][c]
(i)[d]	3.6 ± 0.5	1.9 ± 0.3	1.0 ± 0.2	2.8 ± 0.6	1.6 ± 0.3
(ii)[e]	0.50 ± 0.02	–			
(iii)[f]	1000 ± 300	–			

[a] Observed stability constant referred to Equation (1), Scheme 2. [b] Observed stability constant referred to equation (2), Scheme 2. [c] Rate constants referred to equations (1) and (2), Scheme 2; values calculated by means of the SPECFIT software as explained in the experimental section. [d] Titration of **1**·2PF$_6$ with **CX**. [e] Titration of a solution of $\mathbf{1}^{2+}$ containing an excess of PF_6^- anions with **CX**. [f] Titration of $\mathbf{1}^{2+}$ with a solution of **CX** containing two equivalents of TsO^- anions.

To clarify the titration results, we also constructed several Job plots,[14] by performing the experiments at different concentrations and reading the absorption changes at various wavelengths (see Figure S7 in the Supporting Information). The Job plots show that the molar fraction corresponding to the maximum (or minimum) of the plots depends on the concentration and the wavelength; this result demonstrates that there is more than one type of adduct. Even though these experiments do not fully elucidate the stoichiometry of the complexes, they support the interpretation of the UV/Vis spectroscopic titration.

To confirm the stoichiometry of the host–guest complexes and gain more information on the mechanism of association, we performed kinetic experiments by mixing CH_2Cl_2 solutions of **CX** and **1**·2PF$_6$ in 0.7:1 and 2:1 molar ratios, to favour the formation of the 1:1 and 2:1 complexes, respectively. The kinetic traces recorded by monitoring absorption changes at 421 (see Figure 5) and 338 nm were fitted with the SPECFIT[13] fitting program. The results show that, upon mixing **CX** and **1**·2PF$_6$ in 0.7:1 molar ratio, the 1:1 complex is formed in two steps, namely a second-order association reaction followed by a first-order rearrangement of the adduct (Eq. (1) in Scheme 2).

$$\mathbf{1} + \mathbf{CX} \underset{k_{-1}}{\overset{k_1}{\rightleftharpoons}} [\mathbf{CX}\supset\mathbf{1}]^{\#} \xrightarrow{k_1'} [\mathbf{CX}\supset\mathbf{1}] \qquad (1)$$

$$[\mathbf{CX}\supset\mathbf{1}] + \mathbf{CX} \underset{k_{-2}}{\overset{k_2}{\rightleftharpoons}} [(\mathbf{CX})_2\supset\mathbf{1}] \qquad (2)$$

Scheme 2. Kinetic models used to fit the kinetic traces. The counterions are not reported for reasons of clarity.

Upon mixing **CX** and **1**·2PF$_6$ in 2:1 molar ratio, the best fits were obtained by assuming the reaction sequence illustrated by Equations (1) and (2) in Scheme 2. First, the 1:1 adduct is formed in two steps [Eq. (1)], with the same kinetic rate constants determined in the previous experiment. Successively, this complex reacts with a second calixarene molecule, forming the 2:1 complex with a second-order reaction [Eq. (2)]. The values of the kinetic rate constants are gathered in Table 2.

From these results we can conclude that under the experimental conditions of the UV/Vis spectroscopic measurements **CX** and $\mathbf{1}^{2+}$ can also form a 2:1 host–guest complex, which is not observed in the NMR experiments. The main difference between these measurements is the concentration of the molecular components: the concentration of the examined compounds in the UV/Vis spectroscopic experiments ([**1**·2PF$_6$] $< 3.5\times10^{-5}$ M) was two orders of magnitude lower than that in the NMR measurements. The concentrations that can be used in the UV/Vis spectroscopic experiments are determined by the absorption coefficient of the chromophores, the association constant of the adduct and the low solubility of **1**·2PF$_6$ in CH_2Cl_2. Because compound **1**·2PF$_6$ is a salt, its concentration affects the position of the equilibrium between the tight ion pairs and the dissociated

ions in solution, and therefore the relative abundance of different charged species. Moreover, the calixarene wheel is a heteroditopic receptor,[6,7] which can host cations inside its cavity and complex anions by means of the urea moieties on the upper rim.[15,16] Therefore, we tried to mimic the experimental conditions of the NMR measurements by changing the concentration and the nature of the counteranions of compound $\mathbf{1}^{2+}$. We performed UV/Vis complexation experiments under two paradigmatic conditions: the titration of a solution of $\mathbf{1}^{2+}$, which contained an excess of hexafluorophosphate anions, with **CX** [experiment (ii)], and the titration of $\mathbf{1}^{2+}$ with a solution of **CX** containing two equivalents of tosylate (TsO^-) anions [experiment (iii)]. PF_6^- and TsO^- anions were selected as poorly and strongly H-bonding species, respectively;[16] moreover, TsO^- anions also possess an aromatic moiety, which could be involved in π-stacking interactions with both **CX** and $\mathbf{1}^{2+}$.

Before performing experiments (ii) and (iii), we investigated the effect of the concentration and nature of the anions on the photophysical properties of the DAP-based axle. The absorption and luminescence spectra of compound $\mathbf{1}^{2+}$ did not change in presence of 100 equivalents of tetrabutylammonium hexafluorophosphate ($TBAPF_6$) salt. Despite the lack of spectroscopic evidence, it is likely that $\mathbf{1}^{2+}$ and PF_6^- ions are in equilibrium with the ion-paired salt, and that the excess of PF_6^- ions displaces this equilibrium towards the associated ion pair.[17] On the other hand, the addition of two equivalents of tetraethylammonium tosylate (TEATsO) caused remarkable changes in both the absorption and emission spectra of $\mathbf{1}^{2+}$ (see Figure 6), comparable

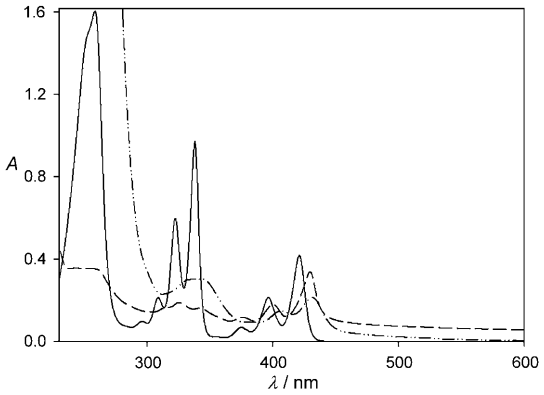

Figure 6. Absorption spectra of compound $\mathbf{1}{\cdot}2PF_6$, 3.3×10^{-5} M (——), upon successive addition of two equivalents of TEATsO (– – –) and two equivalents of **CX**, after 2 days (–·–·–), CH_2Cl_2, RT. Note that addition of TEATsO to $\mathbf{1}{\cdot}2PF_6$ causes precipitation of the salt (see text for details).

to the changes observed upon titration of $\mathbf{1}^{2+}$ with **CX** (see Figure 4). TsO^- ions are more coordinating than PF_6^- ions and can be involved in π-stacking interactions;[16] hence the addition of TEATsO to $\mathbf{1}{\cdot}2PF_6$ led to the exchange of the counterions of the DAP cation, with the formation of the tight ion pair $\mathbf{1}{\cdot}2TsO$. Moreover, soon after the addition of the salt a precipitate started to form, thus preventing any quantitative consideration, but proving that the ion-pairing interactions between $\mathbf{1}^{2+}$ and TsO^- are quite strong. Despite the precipitation of the salt, we noted that the first equivalent of TsO^- ions is responsible for most of the spectroscopic changes. Upon addition of two equivalents of **CX** to this solution, we observed a progressive solubilization of the precipitate, most likely as a consequence of the formation of the inclusion complex; after two days the solution was clear. From a qualitative comparison of the spectra of $\mathbf{1}{\cdot}2TsO$ free and complexed with **CX** (see Figure 6), we observed a further shift towards lower energies of the bands at $\lambda > 350$ nm and an increase and loss of structure of the bands in the range 300–350 nm as a consequence of the inclusion of the axle inside the cavity of the calixarene.

As far as experiments (ii) and (iii) are concerned, we performed the absorption and fluorescence titrations of a solution of $\mathbf{1}{\cdot}2PF_6$ containing 100 equivalents of $TEAPF_6$ with **CX** (Figure S8 in the Supporting Information), and of $\mathbf{1}{\cdot}2PF_6$ with a solution of **CX** containing two equivalents of TEATsO (Figure S9 in the Supporting Information). The spectroscopic changes resemble those obtained in the titration of $\mathbf{1}{\cdot}2PF_6$ with **CX** (see Figure 4). The absorption and luminescence data were best fitted with the SPECFIT program[13] assuming uniquely the formation of a 1:1 host–guest complex. The association constants are gathered in Table 2.

Taken together, the results of experiments (i)–(iii) clearly show that the concentration and nature of the anions affect both the stoichiometry and the stability of the supramolecular adducts formed by $\mathbf{1}^{2+}$ and **CX**. A possible explanation can be found by considering that in this system several equilibria can exist, as summarized in Scheme 3. The horizontal reactions represent the ion-pairing equilibria, which involve the free axle, as well as the 1:1 and 2:1 host–guest com-

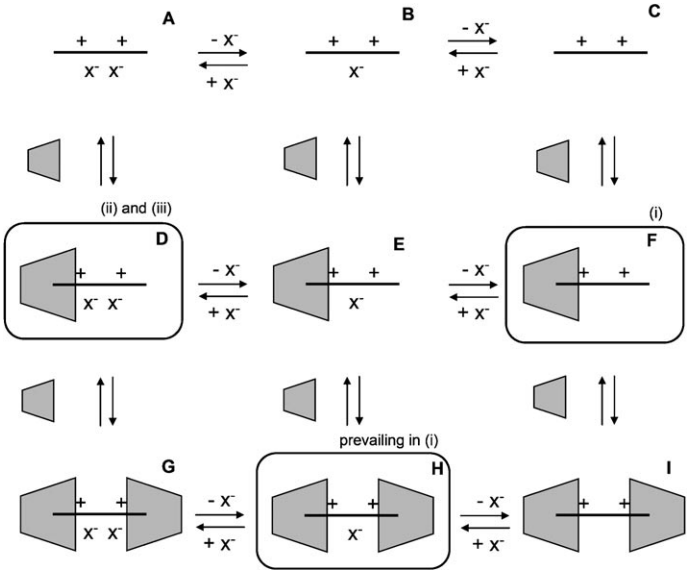

Scheme 3. Equilibria for ion-pair dissociation (horizontal processes) and host–guest association (vertical processes) of the investigated system. Representation of the species in G–I as a threaded complex is hypothetical. See the text for more details.

plexes; because the calixarene is also an anion receptor, these equilibria are obviously influenced by the hydrogen-bonding interactions between the anions and the urea moieties of the wheel. The vertical reactions represent the association equilibria, which involve the axle in its differently ion-paired forms. A quantitative, exhaustive investigation of all these equilibria is not possible with our data, but some reasonable comments can be made.

First of all, the portion of the axle that penetrates the cavity of the calixarene has to be free from its counterions for steric reasons.[15] Molecular models and the results obtained for related complexes[15] indicate that the species involved in the formation of the adducts are most likely the free and one-anion-paired axles (B and C in Scheme 3). It follows that the calculated association constants are apparent values, because they do not take into account the ion-pairing equilibria. The observed stability constants in experiments (ii) and (iii) are one order of magnitude lower and three orders of magnitude larger, respectively, than in experiment (i) (Table 2). As already pointed out, the anions play a dual role. On the one hand, they can interact with the axle, displacing the ion-pairing equilibria towards the associated salt; as a consequence, the "active" monocationic and dicationic species (B and C in Scheme 3) are subtracted from the complexation equilibria (vertical processes in Scheme 3) and the observed association constant is lower than the real one. On the other hand, the anions can interact with the diphenylurea units on the upper rim of the wheel, thus concurring in stabilizing the host–guest complex. In experiment (ii), a solution of **1**·2PF_6 containing 100 equivalents of $TEAPF_6$ was titrated with **CX**; the main effect of these poorly coordinating anions[16] is to displace the ion-pairing equilibria towards the associated salt, and thus the observed stability constant decreases with respect to experiment (i) (Table 2). In experiment (iii), a solution of **1**·2PF_6 was titrated with a solution of **CX** containing two equivalents of TEATsO; TsO^- anions are strongly coordinating,[16] and can interact with both the axle (see above) and the diphenylurea moieties of the wheel through hydrogen-bonding and π-stacking interactions. Under these experimental conditions the wheel, by interacting with TsO^-, seems to be a better host for the axle, at least for two reasons: it bears in the upper rim the TsO^- ions which pre-organize the wheel and exhibit a high coordinating ability towards the axle; moreover, it becomes a negative species. Indeed, the observed stability constant in experiment (iii) is three orders of magnitude larger than in experiment (i).

We can therefore identify three main energetic factors that contribute to the stabilization of the supramolecular complexes: a) the interaction between the axle and the cavity of the wheel, b) the hydrogen-bonding interactions between the urea moieties on the upper rim of the calixarene and the anions, and c) the electrostatic interactions between the cation and the anions held together in the supramolecular structure. In the absence of other effects and if these interactions were additive, it would be expected that the most stable species is [(**CX**)$_2$⊃**1**]·2X (G in Scheme 3), in which the axle is surrounded by two macrocycles and two anions. We have no evidence of the formation of this complex, at least under the majority of the investigated experimental conditions (experiments (ii) and (iii) and NMR experiments).

To explain this behaviour we have to admit that there is competition between the calixarene and the anions for the interaction with the cation, in which steric effects play an important role. From these considerations and a detailed analysis of the spectra, we can infer some information on the identity of the species obtained under different experimental conditions. First of all, to evaluate the extent of the interaction between the axle and the cavity of the wheel, an analysis of the absorption spectra in the region $240 < \lambda < 300$ nm can be very useful. In this region the calixarene makes a substantial contribution to the absorption spectrum, and the encapsulation of a cationic guest inside the wheel considerably affects the absorption spectrum of the calixarene.[15] Therefore, we compared the sum of the spectra of **1**·2PF_6 and **CX** in a 1:2 ratio with the spectrum of a mixture of the molecular components in the same proportion (Figure S10 in the Supporting Information). This comparison revealed that the two spectra are very similar in the region at $\lambda < 300$ nm: such an observation suggests that the cationic portion of the axle is scarcely encapsulated inside the cavity of the wheel, presumably because of the relatively large size of the DAP unit.

In previously studied calixarene systems[6,7,15,18] with a bipyridinium-type axle, the encapsulation is more efficient and there is no evidence of formation of 2:1 host–guest complexes. On the other hand, a bipyridinium unit can indeed form a 2:1 host–guest complex with a calix[4]arene, the small cavity of which affords a less efficient encapsulation.[5i] Additionally, from a comparison of the absorption spectra of the adducts in the three experiments (see Figure 7), we can guess that the 1:1 complex obtained in experiment (i) is different from the 1:1 complex of experiments

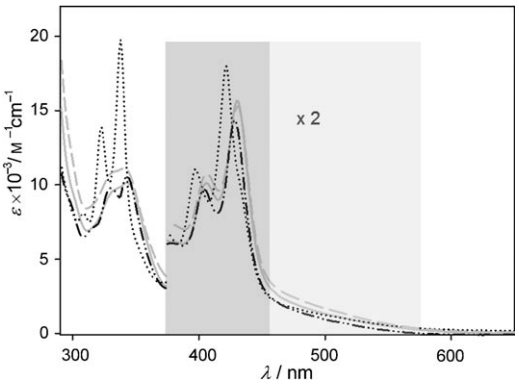

Figure 7. Absorption spectra of the host–guest complexes in CH_2Cl_2, RT: 1:1 (••••, black line) and 2:1 (– – –, grey line) adducts from experiment (i), 1:1 complexes from experiments (ii) (–·–·–, black line) and (iii) (——, grey line). The shaded areas reveal the effects on the absorption spectra that we ascribed to the charge-transfer interaction between the axle and the wheel (light grey) and to the interaction between the anions and the cationic portion of the axle held together in the complex (dark grey).

(ii) and (iii). Both complexes show the absorption tail at $\lambda >$ 450 nm, which is ascribed to a charge-transfer interaction between the electron-accepting DAP unit and the π-electron-rich diphenylurea moieties on the calixarene.[15] Moreover, the spectra obtained in experiments (ii) and (iii) display a shift of the bands in the range 350–450 nm, which can tentatively be assigned to the interaction between the charged axle and the anions held together in the supramolecular structure, as suggested by the shape of the spectrum of the tight ion pair **1**·2TsO (see Figure 7). These differences would suggest that under the dilute conditions of experiment (i) the interaction with the anions is lower than that in experiments (ii) and (iii), and that these adducts differ in the extent of ion pairing between the axle and the anions.

Upon addition of **CX** to the 1:1 adducts, only under the conditions of experiment (i) do we observe the formation of the 2:1 host–guest complex. The absorption spectrum of this species (see Figure 7) shows an increase of the charge-transfer band and a shift towards lower energies of the bands of the transition to the first ππ* excited state ($350 < \lambda <$ 450 nm). These observations would suggest, respectively, that the DAP unit is involved in charge-transfer interactions with the aromatic units of both wheels, and that at least one anion is engaged in the supramolecular complex. Although we do not have direct structural evidence in support of a pseudorotaxane topology for the 2:1 adduct,[19] alternative structures (e.g., the $\mathbf{1}^{2+}$ guest sitting orthogonally to the rims of two wheels without penetrating the respective cavities, or interacting with the calixarene walls in an "alongside" fashion) do not fully account for the observed spectra. The 2:1 adduct cannot interact with two anions, because this would imply that two wheels and two anions can coexist in the supramolecular complex, and therefore complexes with 2:1 stoichiometry (G in Scheme 3) would be expected to form also in experiments (ii) and (iii). From this analysis we can conclude that the 2:1 adduct observed in experiment (i) is the monocationic $[(\mathbf{CX})_2\supset\mathbf{1}]\cdot X^+$ (H in Scheme 3), whereby the axle is surrounded by two wheels and one anion. In experiments (ii) and (iii) this species is not formed, so we conclude that the 1:1 complex observed under these conditions is the neutral species $[\mathbf{CX}\supset\mathbf{1}]$·2X (D in Scheme 3), in which the axle is surrounded by one wheel and two anions are present, thereby preventing the coordination of a second wheel molecule. As far as the 1:1 adduct of experiment (i) is concerned, the absorption spectrum would suggest that this is the dicationic species $[\mathbf{CX}\supset\mathbf{1}]^{2+}$ (F in Scheme 3), the axle of which is surrounded just by one wheel, and it is therefore able to take up a second calixarene.

In summary, the self-assembly of **CX** and the DAP-based axle is a complex phenomenon that involves three types of species (wheel, axle and anions) that can mutually interact. When the species come together, these interactions affect one another because of steric effects and, presumably, also for electronic reasons. The resulting supramolecular structure is determined by the set of interactions that becomes dominant under given experimental conditions: in dilute solutions and with low-coordinating anions, the axle takes two wheels and one anion; in concentrated solutions and in dilute solutions with high-coordinating anions, the axle takes one wheel and two anions.

Conclusion

We have studied a new pseudorotaxane based on a tris(phenylureido)calix[6]arene wheel and a DAP-based cationic axle in apolar solvents. NMR and UV/Vis spectroscopic experiments evidenced the formation of an inclusion complex, in the shape of a pseudorotaxane. The wheel component is a heteroditopic receptor, which is able to complex both the cationic portion of the axle and its counterions. The axle shows characteristic spectroscopic properties that enabled us to investigate the interactions at the basis of the formation of the adducts by means of UV/Vis spectroscopic experiments. This study revealed how the nature of the counterions can affect not only the stability of an adduct, but also its stoichiometry.

Experimental Section

Synthesis: Compounds **CX**[6a] and **1**·2PF$_6$[20] were synthesized according to literature procedures.

NMR diffusion experiments: DOSY experiments were carried out at 293 K on a Bruker Avance 300 spectrometer by using both a stimulated echo[21] and a LED sequence with bipolar gradients. The diffusion coefficient D of the species present in solution was determined by monitoring the intensity decay of at least six resonances in the NMR spectra of the free **CX** in CD_2Cl_2 (10 mM), and of a 2:1 mixture of **CX** and **1**·2PF6 in CD_2Cl_2, as a function of gradient strength applied to the sample. The fitting of the attenuation profiles was carried out by using the equation:

$$I = I_0\exp[-D\gamma^2g^2\delta^2(\Delta-\delta/3-\tau/2)]$$

in which I is the intensity of the observed resonance (attenuated), I_0 the intensity of the reference resonance (unattenuated), D the diffusion coefficient, γ the gyromagnetic ratio, g the gradient strength, δ the gradient pulse length, Δ the diffusion time, and τ the dephasing and rephasing correction time. For each sample 16 experiments were carried out, in which the gradient strength g was varied from 5 to 95% of the maximum gradient intensity (5.35 G mm^{-1}).

ESIMS experiments: Mass measurements were carried out on a Thermo LTQ ORBITRAP XL instrument. The pseudorotaxane mixture in CD_2Cl_2 was diluted one tenth with methanol and filtered. High-resolution mass spectra were recorded in the 0–4000 Da mass range in both positive and negative mode.

Absorption spectra and titration experiments: Measurements were carried out on air-equilibrated CH_2Cl_2 (Merck Uvasol) solutions in the concentration range from 1.0×10^{-5} to 2.5×10^{-4} M. UV/Vis absorption spectra were recorded with either 1 or 5 cm path length cells with a Perkin–Elmer Lambda 45 spectrometer. Titrations were performed by adding with a microsyringe small aliquots (typically 5 μL) of a concentrated (2×10^{-4}–2×10^{-3} M) solution of wheel **CX** to a solution (2.5 mL) of the examined axle species. The UV/Vis absorption changes were monitored throughout the titration. The apparent stability constants of the complexes were calculated by fitting the absorption titration spectra by means of the SPECFIT software using a 1:1 and 2:1 association model.

Stopped-flow absorption experiments: Reaction kinetic profiles were collected on air-equilibrated CH_2Cl_2 (Merck Uvasol) solutions at 293 K with an Applied Photophysics SX 18-MV equipment. The standard flow tube

used had an observation path length of 1.0 cm, and the driving ram for the mixing system was operated at the recommended pressure of 8.5 bar. Under these conditions the time required to fill the cell was 1.35 ms (based on a test reaction). Compounds **CX** and **1**·2PF_6 were mixed in 0.7:1 and 2:1 ratios; the concentration of the axle component after mixing was 2.5×10^{-5} M. As regards the stopped-flow traces, a baseline correction was applied to take into account the dependence of the instrument response on pressure. In all the experiments, the cell block and drive syringes were thermostated by using a circulating constant-temperature bath maintained at the required temperature. The kinetic absorbance curves obtained by mixing **CX** and **1**·2PF_6 in 0.7:1 ratio were analysed for time $t\geq2$ ms with the kinetic model reported in Scheme 2, Equation (1), by means of the SPECFIT fitting program.[13] The kinetic absorbance curves obtained by mixing **CX** and **1**·2PF_6 in 2:1 ratio were also analysed for $t\geq2$ ms with the kinetic model reported in Scheme 2. The data were fitted by means of the SPECFIT fitting program; the values of the kinetic rate constants for the formation of the 1:1 complex were fixed to the values obtained in the previous experiment. The value of the association constant K_2 was fixed to the value obtained in the titration experiments.

Acknowledgements

This research was partly supported by the EU (STREP "Biomach" NMP4-CT-2003-505487), the Italian Ministry of University and Research (FIRB "Manipolazione Molecolare per Macchine Nanometriche" and PRIN "Sistemi Supramolecolari per la costruzione di macchine molecolari, conversione dell'energia, sensing e catalisi") and the Universities of Bologna and Parma. We thank the Centro Interdipartimentale di Misure "G. Casnati" of the University of Parma for mass and NMR measurements.

[1] V. Balzani, M. Venturi, A. Credi, *Molecular Devices and Machines—Concepts and Perspectives for the Nano World*, 2nd ed., Wiley-VCH, Weinheim, **2008**.

[2] a) *Catenanes, Rotaxanes and Knots* (Eds.: J.-P. Sauvage, C. Dietrich-Buchecker), Wiley-VCH, Weinheim, **1999**; b) T. J. Hubin, D. H. Busch, *Coord. Chem. Rev.* **2000**, *200–202*, 5–52; c) E. Mahan, H. W. Gibson in *Cyclic Polymers*, 2nd ed. (Ed.: J. A. Semlyen), Kluwer Publishers, Dordrecht, **2002**, pp. 415–560; d) I. G. Panova, I. N. Topchieva, *Russ. Chem. Rev.* **2001**, *70*, 23–44; e) T. Takata, N. Kihara, Y. Furusho, *Adv. Polym. Sci.* **2004**, *171*, 1–75; f) F. Huang, H. W. Gibson, *Prog. Polym. Sci.* **2005**, *30*, 982–1018; g) G. Wenz, B.-H. Han, A. Mueller, *Chem. Rev.* **2006**, *106*, 782–817; h) J. A. Faiz, V. Heitz, J.-P. Sauvage, *Chem. Soc. Rev.* **2009**, *38*, 422–442; i) J. D. Crowley, S. M. Goldup, A.-L. Lee, D. A. Leigh, R. T. McBurney, *Chem. Soc. Rev.* **2009**, *38*, 1530–1541; j) J. F. Stoddart, *Chem. Soc. Rev.* **2009**, *38*, 1802–1820; k) A. Harada, A. Hashidzume, H. Yamaguchi, Y. Takashima, *Chem. Rev.* **2009**, *109*, 5974–6023; l) Z. Niu, H. W. Gibson, *Chem. Rev.* **2009**, *109*, 6024–6046.

[3] a) C. Reichardt, *Solvents and Solvent Effects in Organic Chemistry*, VCH, Weinheim, **1988**; b) N. Isaacs, *Physical Organic Chemistry*, Longman, Essex, **1987**, pp. 49–55.

[4] a) J. W. Jones, H. W. Gibson, *J. Am. Chem. Soc.* **2003**, *125*, 7001–7004; b) F. Huang, J. W. Jones, C. Slebodnick, H. W. Gibson, *J. Am. Chem. Soc.* **2003**, *125*, 14458–14464; c) T. B. Gasa, J. M. Spruell, W. R. Dichtel, T. J. Sørensen, D. Philp, J. F. Stoddart, P. Kuzmič, *Chem. Eur. J.* **2009**, *15*, 106–116; d) K. Zhu, M. Zhang, F. Wang, N. Li, S. Li, F. Huang, *New J. Chem.* **2008**, *32*, 18271830; e) M. Clemente-León, C. Pasquini, V. Hebbe-Viton, J. Lacour, A. Dalla Cort, A. Credi, *Eur. J. Org. Chem.* **2006**, 105–112.

[5] a) P. D. Beer, P. A. Gale, *Angew. Chem.* **2001**, *113*, 502–532; *Angew. Chem. Int. Ed.* **2001**, *40*, 486–516; b) P. A. Gale, *Coord. Chem. Rev.* **2003**, *240*, 191–221; c) A. Arduini, E. Brindani, G. Giorgi, A. Pochini, A. Secchi, *J. Org. Chem.* **2002**, *67*, 6188–6194; d) C. A. Hunter, C. M. R. Low, C. Rotger, J. G. Vinter, C. Zonta, *Chem. Commun.* **2003**, 834–835; e) A. Casnati, C. Massera, N. Pelizzi, I. Stibor, E. Pinkassik, F. Ugozzoli, R. Ungaro, *Tetrahedron Lett.* **2002**, *43*, 7311–7314; f) V. Böhmer, A. Dalla Cort, L. Mandolini, *J. Org. Chem.* **2001**, *66*, 1900–1902; g) M. Hamon, M. Ménand, S. Le Gac, M. Luhmer, V. Dalla, I. Jabin, *J. Org. Chem.* **2008**, *73*, 7067–7071; h) L. Pescatori, A. Arduini, A. Pochini, A. Secchi, C. Massera, F. Ugozzoli, *CrystEngComm* **2009**, *11*, 239–241; i) L. Pescatori, A. Arduini, A. Pochini, A. Secchi, C. Massera, F. Ugozzoli, *Org. Biomol. Chem.* **2009**, *7*, 3698–3708; j) K. Zhu, S. Li, F. Wang, F. Huang, *J. Org. Chem.* **2009**, *74*, 1322–1328.

[6] a) A. Arduini, F. Calzavacca, A. Pochini, A. Secchi, *Chem. Eur. J.* **2003**, *9*, 793–799; b) A. Arduini, R. Bussolati, A. Credi, G. Faimani, S. Garaudée, A. Pochini, A. Secchi, M. Semeraro, S. Silvi, M. Venturi, *Chem. Eur. J.* **2009**, *15*, 3230–3242.

[7] A. Arduini, F. Ciesa, M. Fragassi, A. Pochini, A. Secchi, *Angew. Chem.* **2005**, *117*, 282–285; *Angew. Chem. Int. Ed.* **2005**, *44*, 278–281.

[8] a) V. Sindelar, M. A. Cejas, F. M. Raymo, A. E. Kaifer, *New J. Chem.* **2005**, *29*, 280–282; b) V. Sindelar, M. A. Cejas, F. M. Raymo, W. Chen, S. A. Parker, A. E. Kaifer, *Chem. Eur. J.* **2005**, *11*, 7054–7059; c) A. H. Flood, A. J. Peters, S. A. Vignon, D. W. Steuerman, H.-R. Tseng, S. Kang, J. R. Heath, J. F. Stoddart, *Chem. Eur. J.* **2004**, *10*, 6558–6564; d) X. Zhang, C. Zhai, N. Li, M. Liu, S. Li, K. Zhu, J. Zhang, F. Huang, H. W. Gibson, *Tetrahedron Lett.* **2007**, *48*, 7537–7541; e) G. Doddi, G. Ercolani, P. Mencarelli, G. Papa, *J. Org. Chem.* **2007**, *72*, 1503–1506.

[9] R. Ballardini, A. Credi, M. T. Gandolfi, C. Giansante, G. Marconi, S. Silvi, M. Venturi, *Inorg. Chim. Acta* **2007**, *360*, 1072–1082.

[10] C. S. Johnson, Jr., *Prog. Nucl. Magn. Reson. Spectrosc.* **1999**, *34*, 203–256, and references therein.

[11] For a general review on the application of DOSY in supramolecular chemistry, please see: Y. Cohen, L. Avram, L. Frish, *Angew. Chem.* **2005**, *117*, 524–560; *Angew. Chem. Int. Ed.* **2005**, *44*, 520–554.

[12] The reduction of the magnitude of the diffusion coefficient measured upon binding (≈17%) is comparable to that found in similar studies in which an α-cyclodextrin was used as a wheel for the formation of pseudorotaxane compounds, see: L. Avram, Y. Cohen, *J. Org. Chem.* **2002**, *67*, 2639–2644.

[13] SPECFIT, Spectrum Software Associates, R. A. Binstead, Chapel Hill, **1996**.

[14] a) P. Job, *Ann. Chim.* **1928**, *9*, 113–203; b) V. M. S. Gil and N. C. Oliveira, *J. Chem. Educ.* **1990**, *67*, 473–478; c) H.-J. Schneider, A. Yatsimirsky, *Principles and Methods in Supramolecular Chemistry*, Wiley, New York, **2000**.

[15] A. Credi, S. Dumas, S. Silvi, M. Venturi, A. Arduini, A. Pochini, A. Secchi, *J. Org. Chem.* **2004**, *69*, 5881–5887.

[16] *Supramolecular Chemistry of Anions* (Eds.: A. Bianchi, K. Bowman-James, E. García-España), Wiley-VCH, Weinheim, **1997**.

[17] a) It is known that in the case of 4,4′-bipyridinium derivatives the addition of an excess of PF_6^- ions to the TsO^- salt causes the exchange of the counterions, see: ref. [15]; b) In this case we could not perform the experiment on **1**·2TsO because of precipitation.

[18] A. Arduini, R. Bussolati, A. Credi, A. Pochini, A. Secchi, S. Silvi, M. Venturi, *Tetrahedron* **2008**, *64*, 8279–8286.

[19] Any attempt to obtain crystals of the 2:1 adduct suitable for X-ray analysis failed.

[20] A. J. Blacker, J. Jazwinski, J.-M. Lehn, *Helv. Chim. Acta* **1987**, *70*, 1–12.

[21] D. Wu, A. Chen, C. S. Johnson, Jr., *J. Magn. Reson. Ser. A* **1995**, *115*, 123–125.

Received: November 5, 2009
Revised: January 4, 2010
Published online: February 8, 2010

